Supporting Information for

Simultaneous Single-Cell Analysis of Na^+, K^+, Ca^{2+} and Mg^{2+} in Nervous Cells in a Microfluidic System

Lu Li, Yuanyuan Fan, Qingling Li, Renjie Sheng, Haibin Si, Juan Fang, Lili Tong, Bo Tang*

College of Chemistry, Chemical Engineering and Materials Science, Collaborative Innovation Center of Functionalized Probes for Chemical Imaging in Universities of Shandong, Key Laboratory of Molecular and Nano Probes, Ministry of Education, Institute of Molecular and Nano Science, Shandong Normal University, Jinan, 250014, P.R. China.

Author Email: tangb@sdnu.edu.cn
Fax: 86-531-86180017

Table of contents

1. The sampling process based on consecutive gated injection.

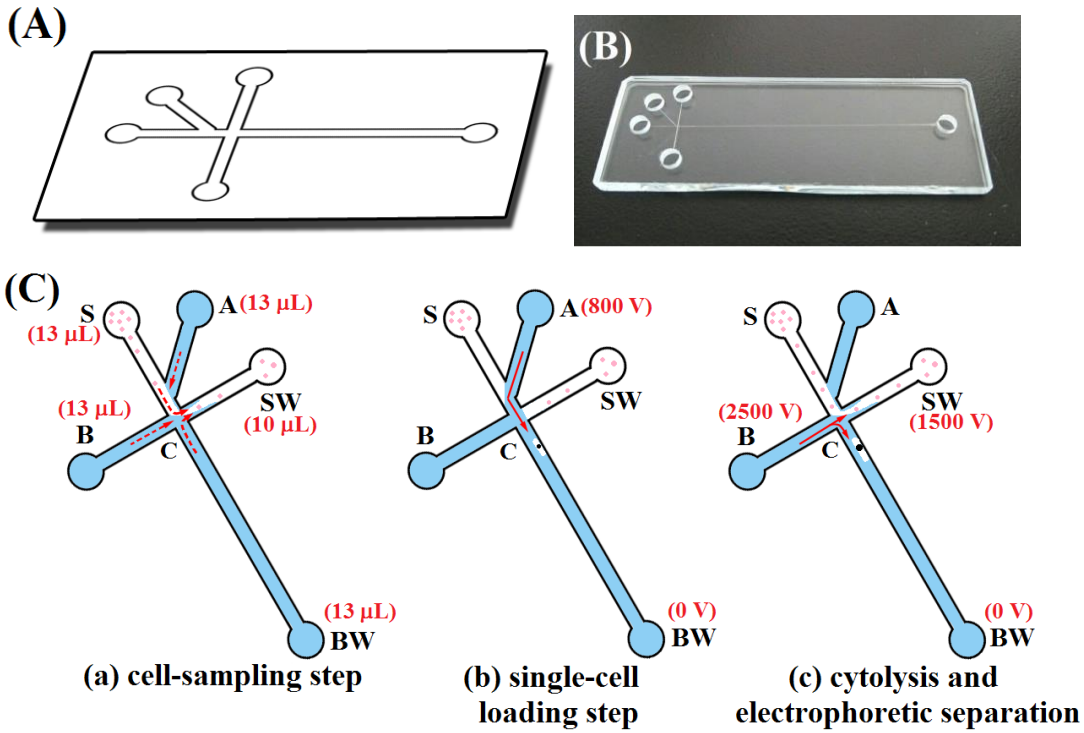

Figure S1. (A) The schematic diagram of the five-reservoir microchip. (B) The photos of the five-reservoir microchip. (C) The sampling process based on consecutive gated injection. (a), cell-sampling step; (b), single-cell loading step; (c), cytolysis and electrophoretic separation step.

Prior to the experiment, buffer (B), buffer waste (BW) and auxiliary (A) reservoirs were all filled with 13 μL of electrophoresis running buffer, the sample waste (SW) reservoir was filled with 10 μL of electrophoresis running buffer and the sample reservoir (S) was filled with 13 μL of cell suspensions (5×10^5 cells/mL). Four Pt-electrodes were inserted into the reservoirs (B, BW, A and SW). Specifically, in the cell-sampling step, single cells in reservoir S entered into the sample channel, S–C, and flowed toward reservoir SW (Figure C a) because of hydrostatic pressure. Then, 800 V was applied to the auxiliary reservoirs A for 1 s. While the BW reservoir was grounded, one cell was loaded into the separation channel, C–BW (Figure C b). Next, the electricity was switched to the five reservoirs with B, SW, and BW at 2500, 1500, and 0 V, respectively, and with A and S floating for 44 s. At this time, cytolysis and electrophoretic separation were immediately conducted (Figure C c).

2. The reactions of the fluorescent probes with four different ions.

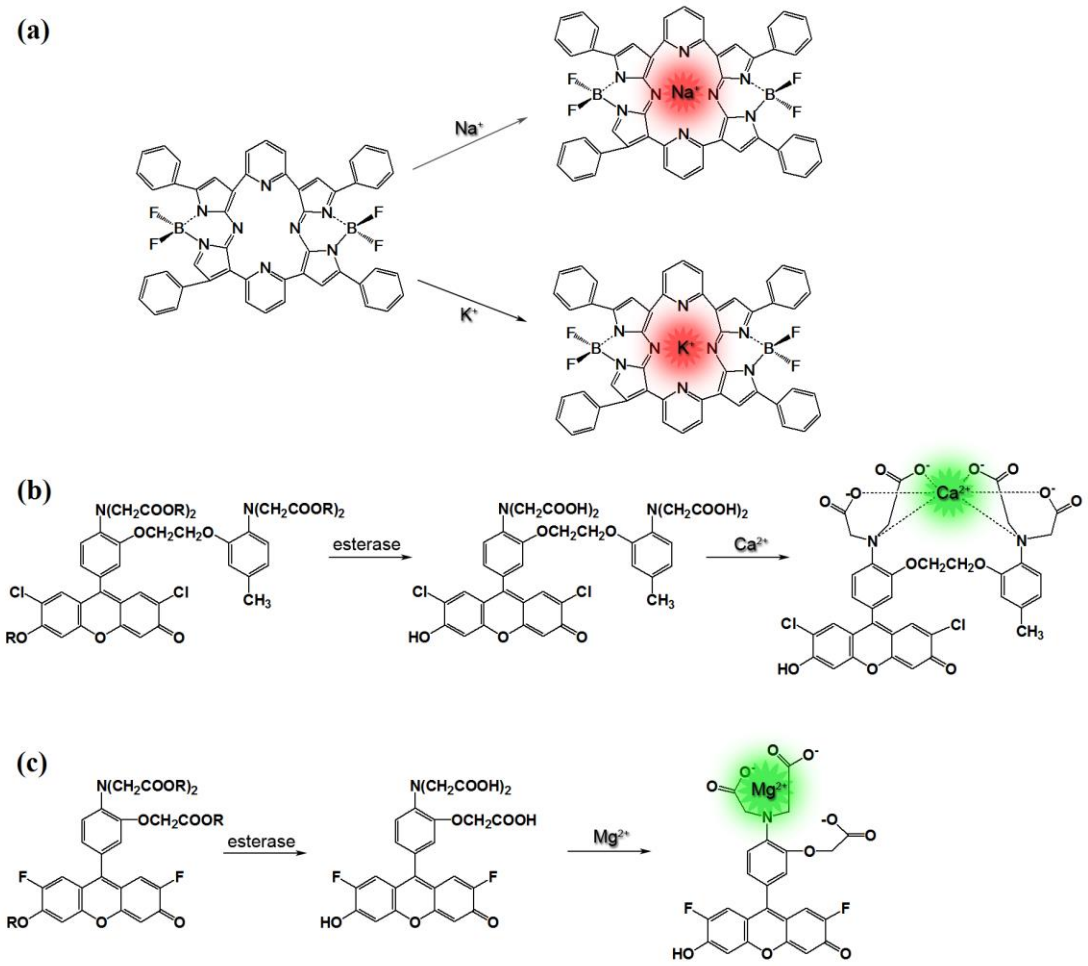

Figure S2. The reactions of cBDP with Na^+ and K^+ (a), Fluo-3 AM with Ca^{2+} (b), and Mag-Fluo-4 AM with Mg^{2+} (c).

3. Excitation and emission spectra of the fluorescent probes with the four metal ions.

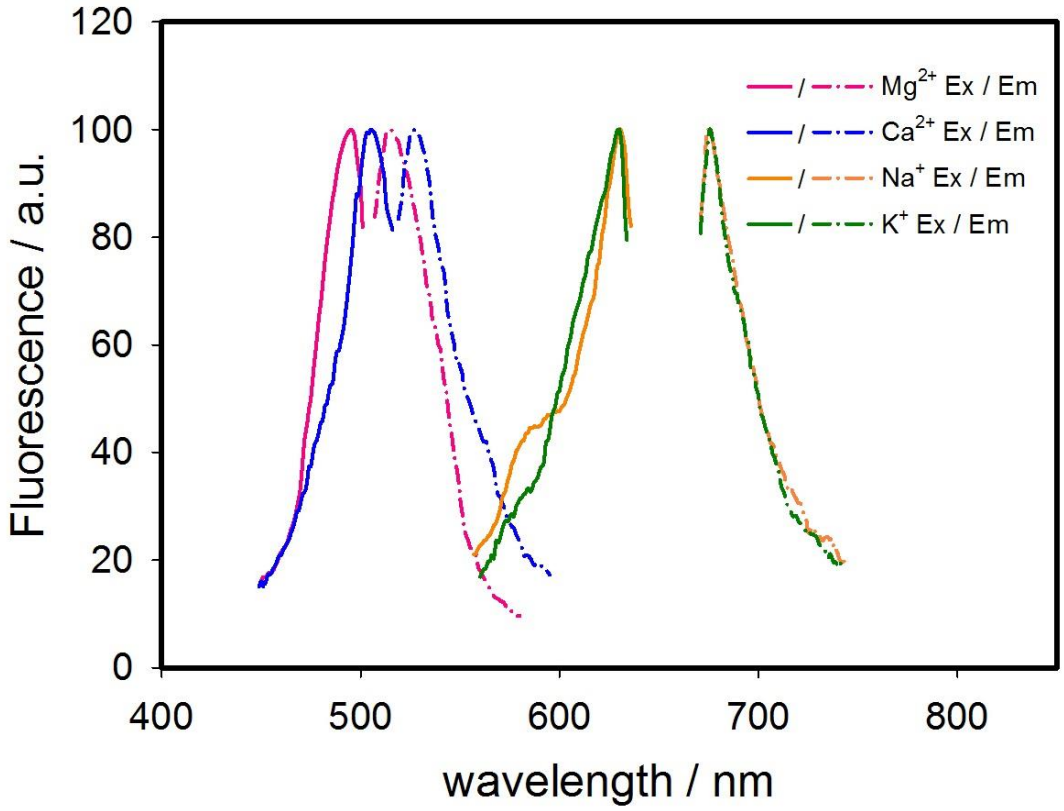

Figure S3. The excitation and emission spectra of cBDP with Na^+ or K^+, Fluo-3 AM with Ca^{2+} and Mag-Fluo-4 AM with Mg^{2+}. The four ions were separately mixed with 60 μM cBDP, 5 μM Fluo-3 AM and 5 μM Mag-Fluo-4 AM. The excitation and emission wavelength of the three probes and the corresponding laser and collected wavelength range are shown in Table 1.

Table S1. The selected laser and collected wavelength range for the different excitation (Ex) and emission (Em) wavelengths.

Metal ions	Ex / nm	Em / nm	Laser / nm	Collected wavelength / nm
K^+	630	676	633	695±15
Na^+	630	675		
Ca^{2+}	505	527	473	525±15
Mg^{2+}	495	515		

4. Selectivity of fluorescent probes for various metal ions.

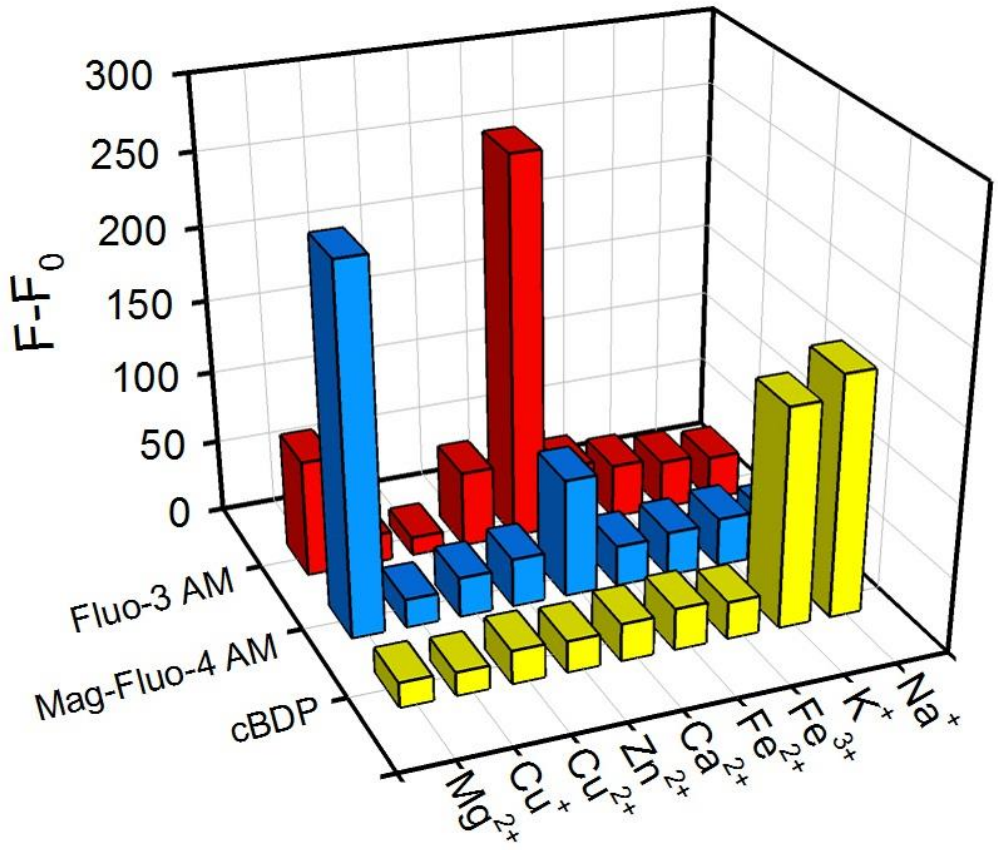

Figure S4. Selectivity of the cBDP, Mag-Fluo-4 AM and Fluo-3 AM probes for various metal ions. The fluorescence intensity was measured using metal ion-containing solutions (100 μM) incubated with 5 μM Fluo-3 AM (red), 5 μM Mag-Fluo-4 AM (blue) and 60 μM cBDP (yellow) respectively.

5. Analytical performance of the proposed Method.

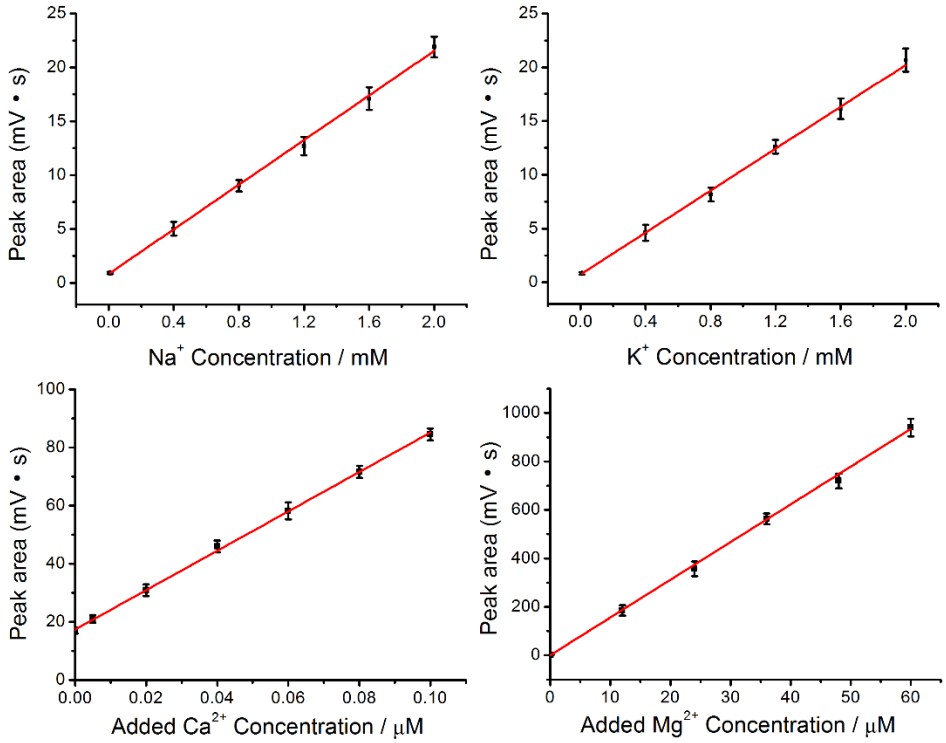

Figure S5. The calibration curves of Na^+, K^+, Ca^{2+} and Mg^{2+}. The concentrations of the Na^+ and K^+ standard solutions are 0.008 mM, 0.4 mM, 0.8 mM, 1.2 mM, 1.6 mM, 2 mM. The added Ca^{2+} concentrations of standard solutions are 0.005 μm, 0.02 μm, 0.04 μm, 0.06 μm, 0.08 μm, 0.1 μm and the added Mg^{2+} concentrations of standard solutions are 0.1 μm, 12 μm, 24 μm, 36 μm, 48 μm, 60 μm.

Table S2. Linearity, reproducibility of migration time and peak area, and LODs for Na^+/K^+-cBDP, Ca^{2+}-Fluo-3 AM and Mg^{2+}-Mag-Fluo-4 AM.

Metal ions	Linerity range	Regression equation	R^2	RSD (%,n=6) (migration time)	RSD (%,n=6) (peak area)	LODs
Na^+	0.008-2 (mM)	Y=0.833+10.2X (linear concentration curve) [a]	0.9993	0.60	3.2	0.293 fmol
K^+	0.008-2 (mM)	Y=0.707+9.69X (linear concentration curve) [a]	0.9992	0.53	2.9	0.316 fmol
Ca^{2+}	0.005-0.1 (μM)	Y=18.1+669X (linear concentration curve) [b]	0.9992	0.72	3.3	0.158 amol
Mg^{2+}	0.1-60 (μM)	Y=0.987+15.2X (linear concentration curve) [b]	0.9991	0.68	3.5	3.16 amol

[a] Y: peak area in mV s; X: concentration of the analyte in mM.

[b] Y: peak area in mV s; X: concentration of the analyte in μM.

The metal ions concentrations were quantified according to a linear equation from the calibration curves. Firstly, the fluorescence intensities of the four metal ions with different concentrations (Na^+, 0.008-2 mM; K^+, 0.008-2 mM; Ca^{2+}, 0.005-0.1 μM; Mg^{2+}, 0.1-60 μM) were measured. Then, four calibration curves with the peak areas as Y–axis and the concentrations of the metal ions as X-axis were obtained. For the single-cell quantitation, after the cell lysis, the fluorescence signals of the single cells were measured, the metal ions concentrations C_{metal} in the injection volume V_{inj} were calculated according to the linear equation from the calibration curves. The V_{inj} was measured to be 206 pL, which was considered as the volume of standard Na^+-cBDP solution in the microchannel when a detection in homogeneous solution with Na^+-cBDP was performed by the proposed sampling method. The amount of the metal ions n_{metal} in single cells were calculated according to the formula $n_{metal}=C_{metal}\times V_{inj}$. The concentrations of metal ions in single cells were obtained by multiply n_{metal} by an approximate cell volume 10 pL.

6. Concentration distribution profiles of the four ions in untreated PC-12 cells, pinacidil-treated PC-12 cells and nifedipine-treated PC-12cells.

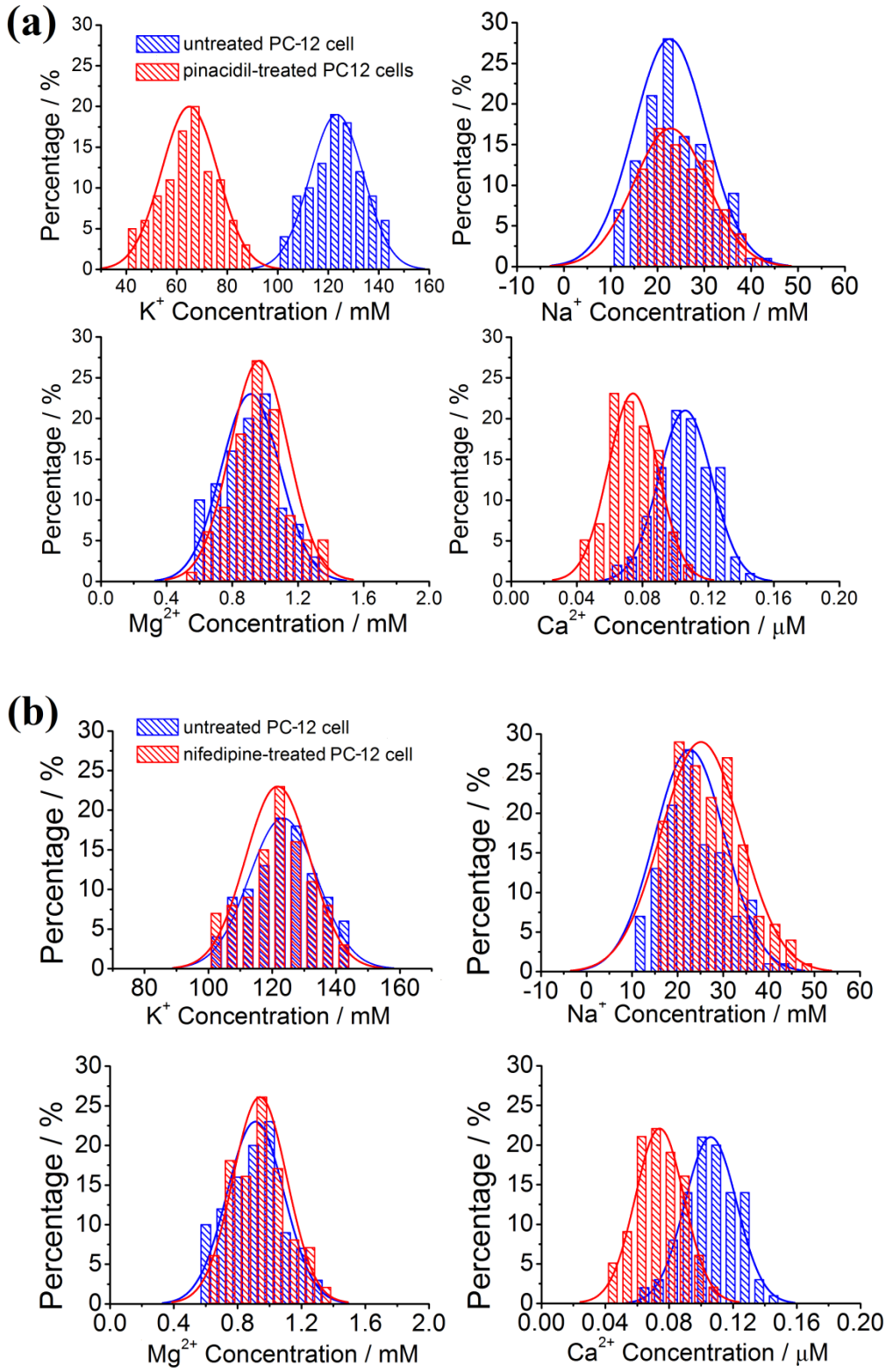

Figure S6. The concentration distribution profile of Na^+, K^+, Ca^{2+} and Mg^{2+} in 100 normal PC-12 cells and 100 pinacidil -treated PC-12 cells (A), in 100 normal PC-12 cells and 100 nifedipine-treated PC-12 cells (B).

7. Cell viability of the Aβ$_{25-35}$-treated cells.

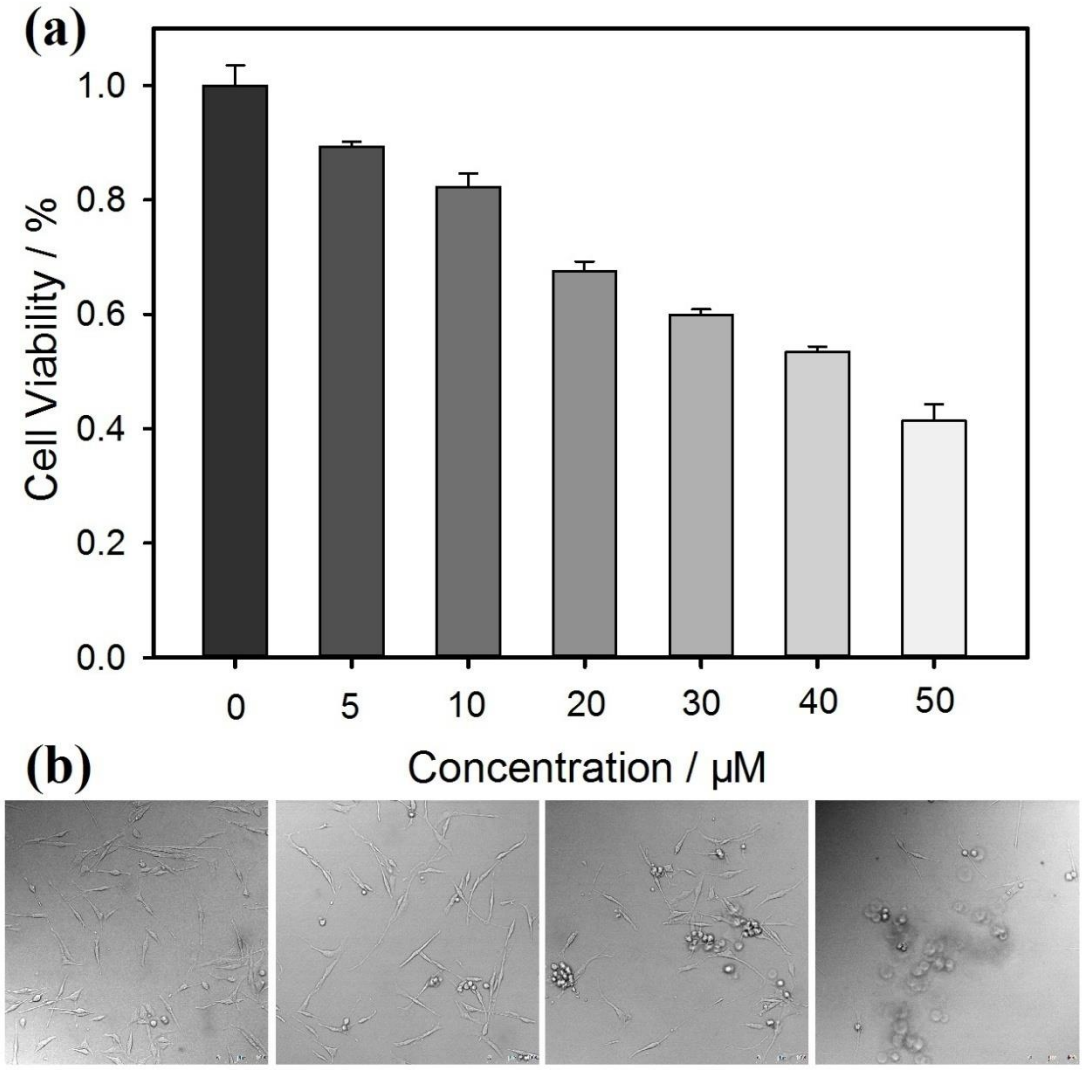

Figure S7. Cell viability assay and morphologic changes of Aβ$_{25-35}$ treated PC-12 cells: (a), the concentrations of Aβ$_{25-35}$ were 0 μM, 5 μM, 10 μM, 20 μM, 30 μM, 40 μM and 50 μM. Decreased cell viability occurred at higher Aβ $_{25-35}$ concentrations; (b), morphologic changes of Aβ$_{25-35}$-treated PC-12 cells. The concentrations of Aβ$_{25-35}$ were 0 μM, 10 μM, 20 μM and 50 μM from left to right.

8. Concentrations of the four ions in Aβ$_{25-35}$-treated PC-12 cells and untreated PC-12 cells.

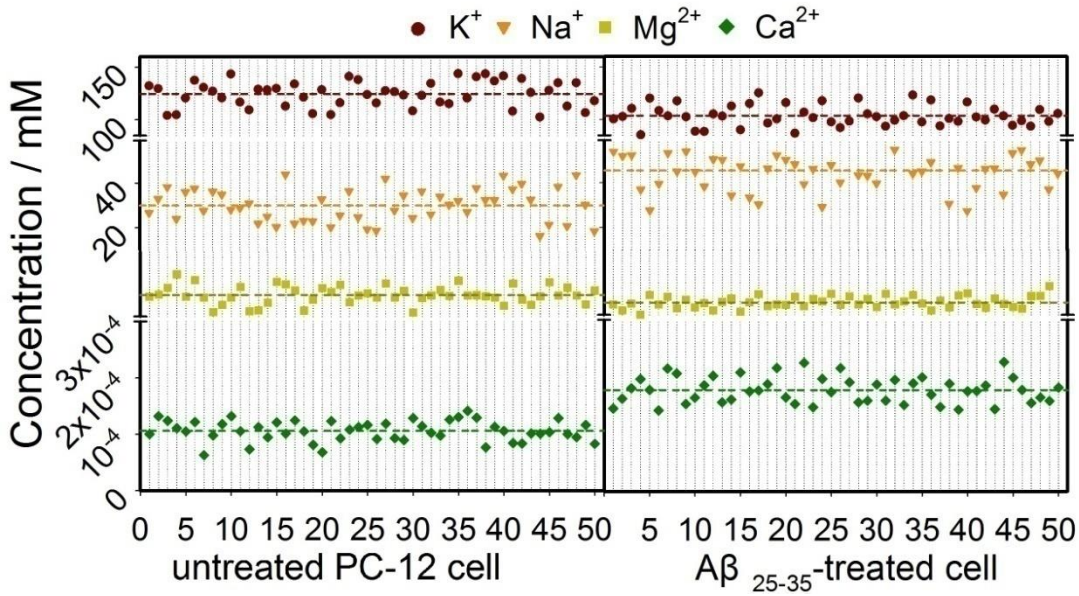

Figure S8. The concentrations of Na^+, K^+, Ca^{2+} and Mg^{2+} in 50 individual untreated PC-12 cells and 50 individual Aβ$_{25-35}$-treated PC-12 cells.

9. P-value calculated from the Shapiro-Wilk test

Table S3. P-values calculated from the Shapiro-Wilk test of the four metal ions concentrations at pretreatment and posttreatment.*

Cells	P-value (K^+)	P-value (Na^+)	P-value (Ca^{2+})	P-value (Mg^{2+})
Untreated PC-12 cells	0.1206	0.3747	0.3530	0.1607
Pinacidil-treated PC-12 cells	0.2145	0.1643	0.3015	0.4802
Nifedipine-treated PC-12 cells	0.07669	0.6153	0.3601	0.07491
$A\beta_{25-35}$-treated PC-12 cells	0.1774	0.7374	0.7742	0.2765

*All the P-values are greater than 0.05, indicating that all the concentrations of the four metal ions obey the normal distribution.

10. Na^+/K^+-ATPase activity assay.

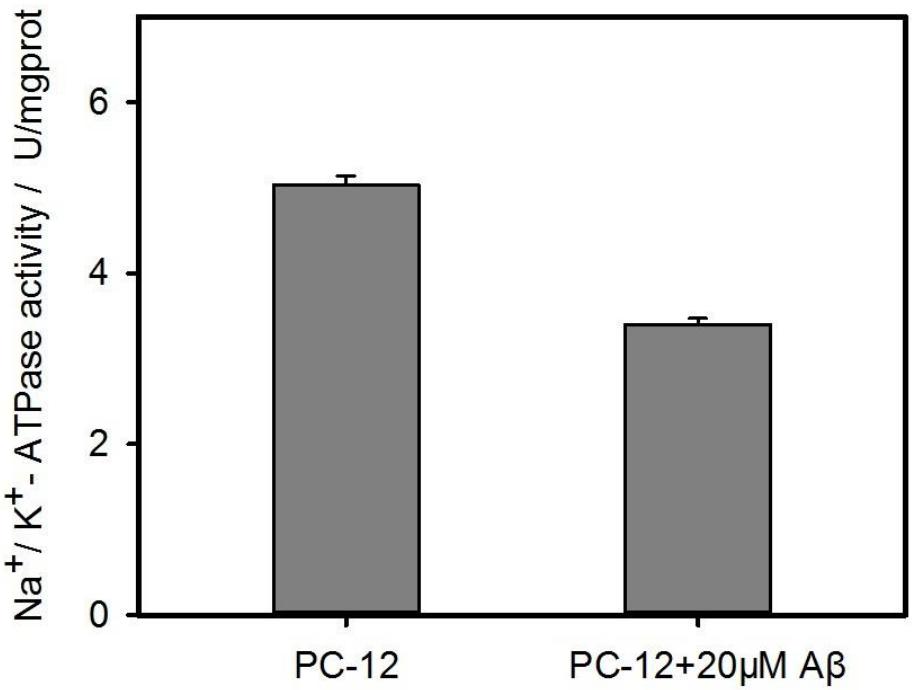

Figure S9. Na^+/K^+-ATPase activity assay. The Na^+/K^+-ATPase activity was reduced following the exposure to $A\beta_{25-35}$.

11. Apoptosis Assay.

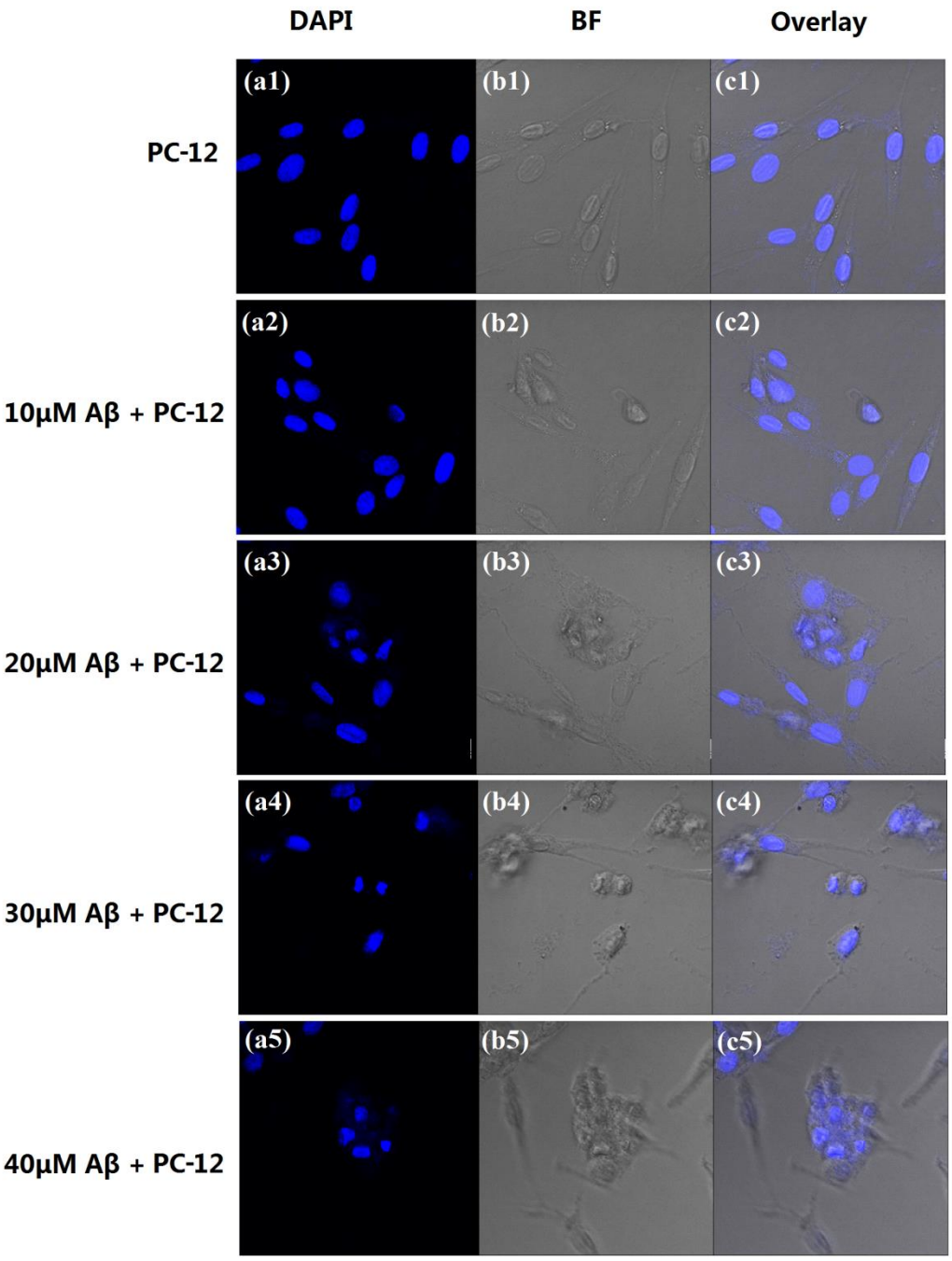

Figure S10. Apoptosis verification assay.